Spatiotemporal variability of CO$_2$, N$_2$O and CH$_4$ fluxes from a semi-deciduous tropical forest soil in the Congo basin

Roxanne Daelman[1,2], Marijn Bauters[2], Matti Barthel[3], Emmanuel Bulonza[4], Lodewijk Lefevre[1,2], José Mbifo[5], Johan Six[3], Klaus Butterbach-Bahl[6,7], Benjamin Wolf[7], Ralf Kiese[7], Pascal Boeckx[1]

[1]Isotope Bioscience Laboratory (ISOFYS), Department of Green Chemistry and Technology, Ghent University, Ghent, Belgium
[2]Q-Forest lab, Department of Environment, Ghent University, Ghent, Belgium
[3]Department of Environmental System Science, ETH Zurich, Zurich Switzerland
[4]Ecole Régionale d'Aménagement et Gestion Intégrés des Forêts et Territoires tropicaux (ERAIFT), Kinshasa, Democratic Republic of Congo
[5]Institut National pour l'Etude et la Recherche Agronomiques (INERA), Yangambi, Democratic Republic of Congo
[6] Land-CRAFT, Department of Agroecology, Aarhus University, Aarhus, Denmark
[7]Institute of Meteorology and Climate Research, Atmospheric Environmental Research (IMK-IFU), Karlsruhe Institute of Technology, Garmisch-Partenkirchen, Germany

Correspondence to: Roxanne Daelman (Roxanne.Daelman@Ugent.be)

Abstract. Tropical forests play an important role in the greenhouse gas exchange between biosphere and atmosphere. Despite holding the second largest tropical forest globally, the Congo basin is generally understudied and ground based greenhouse gas flux data are lacking. In this study, high frequency measurements spanning of sixteen months from automated and manual fast box soil chambers are combined, to characterize spatio-temporal variability in soil greenhouse gas fluxes from a lowland tropical forest in Yangambi, in the Congo Basin. Based on sub-daily continuous measurements, for CO$_2$, a total emission of 15.3 ± 4.4 Mg C ha^{-1} yr^{-1} was calculated, with highest fluxes at the start of the wetter periods and a decline in emissions during drier periods. For CH$_4$, the total uptake was -3.9 ± 5.2 kg C ha^{-1} yr^{-1}. Over the whole period the soil acted as a sink however sporadic emission events were also observed. For N$_2$O an emission of 3.6 ± 4.1 kg N ha^{-1} yr^{-1} was calculated, which is higher than most previously reported tropical forest estimates. N$_2$O emissions decreased substantially during drier periods and emission pulses were detected after rain events. High spatial and temporal variability was observed for both CH$_4$ and N$_2$O, but less for CO$_2$. Higher spatial variability was assessed by the manual compared to the automated measurements. Overall, the tropical forest soil acted as a major source for CO$_2$ and N$_2$O and a minor sink for CH$_4$.

1 Introduction

The three most important biogenic greenhouse gases (GHG) are carbon dioxide (CO$_2$), methane (CH$_4$), and nitrous oxide (N$_2$O). Although the increase in atmospheric concentrations of these key GHG since 1750 is unequivocally attributed to human activity (IPCC, Calvin et al., 2023), natural ecosystems also contribute significantly to atmospheric GHG budgets. Tropical forests play an important role in the GHG exchange between the biosphere and the atmosphere. Soils are the

dominant terrestrial source of CO_2 and emissions from tropical forest soils are generally higher than from any other vegetation type, due to high soil moisture and temperature (Raich et al., 2002), higher gross primary production (GPP) of tropical forests compared to other forests and the larger proportion of GPP used for autotrophic respiration (Anderson-Teixeira et al., 2016). Soils can both produce and consume CH_4, but globally soils are the largest biotic sink for atmospheric CH_4. Aerobic forest soils consume more CH_4 than other ecosystems, but can become a source when inundated (Dalal et al., 2008; Dutaur et al., 2007). Considering all natural sources of N_2O, soils are the largest contributor. In particular, emissions from tropical forest soils are 50% higher than the global average for soils (Tian et al., 2020), as these tropical forests are generally N rich systems (Brookshire et al., 2012; Hedin et al., 2009). Taking all biogenic GHG together, the net global warming potential of tropical forest systems, suggests to be a small sink (Dalal et al., 2008), but large uncertainties remain as the spatial and temporal variability of tropical forest soil fluxes still remain poorly understood (Arias-Navarro et al., 2017; Courtois et al., 2019).

The difficulty of understanding the dynamics of soil fluxes lies in the multitude of controlling environmental factors and the complexity of the biological and physical mechanisms which lead to a high spatial and temporal variability (Courtois et al., 2018; Vargas et al., 2011). To date, the majority of soil flux measurements have been carried out using manual static chambers; a technique that is able to capture spatial variability up to a certain degree but is labour-intensive and time-consuming. In addition, measurements are generally taken on weekly to monthly time intervals, thus not covering diurnal patterns and resulting in a lower accuracy than higher frequency measurements (Barton et al., 2015). Also, no responses to precipitation events or nocturnal measurements will be present (Courtois et al., 2019; Vargas et al., 2011). Automated soil chambers, on the other hand, allow to capture both diurnal and seasonal variability and even detect short term variations or responses to rapidly changing environmental conditions. Nevertheless, a small number of chambers reduces the spatial scale of the measurements, leading to large uncertainties in the quantification of landscape GHG fluxes (Wangari et al., 2022). Combining automated chambers with fast box measurements can address both the spatial and temporal variability of soil GHG fluxes. However, the complexity of such setup has limited its application in remote environments such as tropical forests, particularly in Africa.

Despite being the second largest tropical forest, the Congo Basin is generally understudied (Malhi et al., 2013). Recent studies show that the climatic conditions in the Congo Basin are already changing with an increasing length of the dry season (Jiang et al., 2019), warming (Dezfuli, 2017; Kasongo Yakusu et al., 2023) and increasing numbers of extreme warm days and nights (Aguilar et al., 2009; Chaney et al., 2014; Kasongo Yakusu et al., 2023) and increasing precipitation intensity (Kasongo Yakusu et al., 2023). Climate change projections suggest that these trends will persist in the future (Karam et al., 2022; Kendon et al., 2019). As soil moisture and temperature are main drivers of soil GHG flus dynamics, these shifts will directly affect the GHG budget (Ni et al. 2018). Quantifying soil fluxes and understanding the role of temperature and moisture as drivers is key to assessing the future response of this biome to climate change. So far only a handful of studies

have reported *in situ* soil flux measurements from the Congo Basin (Fig. S1 and Table S1). Studies such as Barthel et al. (2022), combine biweekly measurements from long-term observation sites, with short-term daily measurement campaigns. However, to calculate more robust GHG budgets and to understand variability, data with a higher spatio-temporal resolution are needed.

In this study, a combination of automated and manual fast box chamber measurements were used, to quantify and understand the spatio-temporal variability of soil GHG fluxes in a semi-deciduous tropical forest in the Congo Basin. The objectives of the study are 1) to quantify annual budgets of soil CO_2, CH_4 and N_2O fluxes, 2) to evaluate the role of soil moisture and temperature as main drivers of these GHG fluxes, and 3) to analyse the spatio-temporal variability of soil GHG fluxes.

2 Methods

2.1 Study site

The study was conducted at the CongoFlux station (0°48′52.0″ N 24°30′08.9″ E) (Fig. S2) (Sibret et al., 2022), located in Yangambi on the right bank of the Congo River, app. 100 km northwest of Kisangani, in the Tshopo Province of the Democratic Republic of Congo (DRC). The site is located in a semi-deciduous, lowland mixed-species forest with strongly weathered, sandy clay loam and poorly drained soils, dominated by Haplic Ferralsols (Gilson et al., 1956; Sibret et al., 2022, Fig S10). The soil in the top 30 cm has an average bulk density (BD) of 1.18 g cm^{-3}, a pH-H_2O of 4.0, with a clay, sand, and silt mass percentage of respectively 30 %, 68 % and 2 %. The average C content is 1.3 % and the average N content is 0.22 % (Table S2). The region has a warm and humid climate with a bimodal rain regime where two dry seasons (Dec-Feb and June-July) alternate with two wet seasons (March-May and August-November) (Kasongo Yakusu et al., 2023). The region experiences a mean annual rainfall of 1822.19 ± 214.80 mm and has a mean annual temperature of 25.0 ± 0.30 °C (Likoko et al., 2019). Within the CongoFlux site, four permanent forest plots of 1 ha (Fig. S2) have been installed according to the RAINFOR-Gem field protocol (Marthews et al., 2013).

2.2 Climatic variables

Half-hourly precipitation at the site was measured by a tipping bucket (ARG100, Campbell scientific Inc., Logan, Utah, USA) installed at 56 m on the tower used for eddy covariance measurements at the study site. Air temperature was measured using temperature and relative humidity sensors (HC2S3, Campbell scientific Inc., Logan, Utah, USA) installed at 2 m height at the tower. Due to high lightning intensity at the site, power outages were frequent, resulting in several data gaps during the measurement period. Close toAt each automated chamber location, two water content reflectometers were installed (CS650, Campbell Scientific Inc., Logan, Utah, USA). The sensors were installed at a depth of 5 cm and 15 cm, at a

distance of around 0.5 m from the collars to avoid disturbance of the soil in the chambers. Every minute the volumetric water content (VWC), soil temperature and electrical conductivity were logged. WFPS was then calculated following equitation 1.

$$WFPS = 100 \times VWC \times \left(1 - \frac{BD}{2.65}\right)^{-1} \quad (1)$$

100 Note: there is a large data gap from the end of March up to the middle of July 2023, due to technical problems with the data logger.

2.3 Measurements of soil CO_2, CH_4 and N_2O exchange

2.3.1 Automated chamber measurements

At the CongoFlux site, nine custom-made dynamic automated chambers (Karlsruhe Institute of Technology) were installed
105 just outside ~~in~~ the 1 ha GEM plot CF1 (Fig. S2). The opaque chambers (0.5 m x 0.5 m x 0.15 m, length, width, and height) were controlled by a central steering unit consisting of a valve-tubing system connecting chambers to two portable analysers, one measuring CO_2 and CH_4 (LI7810, LI-COR inc., Lincoln, Nebraska, USA) and the other measuring N_2O (LI7820, LI-COR inc., Lincoln, Nebraska, USA) concentrations. The nine chambers were placed randomly around the control unit at a distance of maximum 20 m. For each chamber two collars were inserted 10 cm into the soil and chambers were relocated
110 from one collar to the other every two or three weeks. Only chamber 6 was never relocated during the measurement period due to limited cable length. The chamber headspace air was circulated from the chamber to the analysers and back to the chamber with 1/8 inch stainless steel tubing. Before the analysers sample air was dried to constant water vapour with a Nafion dryer. A portable computer was used for steering the valve system for consecutive chamber sampling, closing and opening chambers as well as data acquisition and storage.
115 The chambers were installed in May 2022 and were operated with a closure time of fifteen minutes per flux measurement, followed by two minutes of purging with ambient air, resulting in one datapoint every seventeen minutes. The flux rate was calculated using a linear fit. Measurements of CO_2, CH_4 and N_2O were discarded if the R^2 of the CO_2 measurement was smaller than 0.9, and measurements of N_2O were also discarded if the R^2 of the N_2O measurement was smaller than 0.7, as these values indicated a systematic error such as imperfect closure of the chamber or a technical issue with the analysers.
120 Fluxes with unit mass C h^{-1} m^{-2} for CO_2 and CH_4 and mass N h^{-1} m^{-2} for N_2O were than calculated using equation 2, which is a combination of the ideal gas law and scaling variables:

$$Flux = \frac{dq}{dt} \times \frac{\cancel{60 \times}V \times P \times M_w}{R \times T \cancel{\times A \times 1000}} \times \frac{60}{A \times 1000} \quad (2)$$

With $\frac{dq}{dt}$ the change in mixing ratio over time [ppb minute^{-1} or ppm minute^{-1}] , resulting from the ~~exponential~~linear fit, V the chamber volume [m³], P the long term average air pressure of the site [Pa], $M_w = 12$ for CO_2 and CH_4 and $M_w = 28$ for N_2O
125 [g mol^{-1}], T the average temperature during closure time [°K], A the surface area of the chamber [m²] and R the universal gas constant [J mol^{-1} °K^{-1}]. The data presented in this paper starts from the first of June 2022 ~~up~~until the 26th of September 2023, resulting in a coverage of sixteen months and 25 209 data points for CO_2 and CH_4 and 18 635 data points for N_2O equally

divided between nighttime and daytime measurements. During precipitation events, the automated chambers continued to measure without interruption.

2.3.2 Fast box measurements

The low number of automated chambers limited the spatial coverage of the soil flux measurements. Hence, the fast box method was included to reference the results of the automatic chambers into the larger study area. The four GEM plots on the CongoFlux site were divided into twenty-five subplots of 20 m by 20 m subplots and in each subplot, one soil chamber was installed in March 2023 to be measured using with the fast box method (Hensen et al., 2013; Wangari et al., 2022). The chambers were PVC tubes with a diameter of 5.5 cm and a height of 13 cm, permanently inserted 3 cm into the soil. The four plots CF1, CF2, Mi2 and Mi5 were equipped with twenty-five chambers each, but three chambers were lost (two in Mi2 and one in Mi5) and two locations were measured incorrectly (one in CF2 and one in Mi2), leaving a total of ninety-five chambers. During a period of three weeks from August 4 to August 28, 2023, flux measurements of CO_2, CH_4 and N_2O were made during daytime (between 08:00 – 18:00) in these plots using two portable analysers, one measuring CO_2 and CH_4 (LI7810, LI-COR inc., Lincoln, Nebraska, USA) and one measuring N_2O (LI7820, LIC-COR inc., Lincoln, Nebraska, USA). Plots CF1, CF2 and Mi5 were each measured six times during this three-week period and plot Mi2 only five times. Two plots were measured per day with an average of 5 minutes between consecutive chamber measurements. The plots To avoid consistently measuring the same chamber on the same time of day, the order in which the plots were measured was alternated and at different times of the day, taking care to change the route from chamber to chamber within one plot was changed every session. A closure time of two minutes was used, and the flux rate was calculated using a linear fit and equation 2. The quality control of these fluxes was similar to that of the automated fluxes, with the addition that fluxes with a low R^2 (< 0.7) were also individually checked for their quality. Low R^2 could be due to a low flux and then the flux was put to 0. If the low R^2 was due to fluctuating concentrations, the measurement was discarded. The size of the fast box chambers was smaller than the automated chambers and the number of chambers was larger, so the variation of the fluxes from the fast box chambers would likely be larger than that of the automated chambers. However, as the processing of the fast box data was the same as for the automated fluxes, we believe that the methods are compatible and we therefore can use the automated fluxes for budget calculation and the fast box measurements for referencing the spatial variability without any normalization or correction (Fig S11). No additional climatic variables or soil properties were measured in the four GEM plots.

3 Statistical Analysis

For the automated chambers, the average flux was calculated as the arithmetic mean of all measurements from all chambers and the average fluxes per chamber location were calculated by taking the arithmetic mean of all measurements from each chamber location separately. The coefficient of variation (CV) for each chamber location was calculated as the standard

deviation (SD) of the chamber location divided by the arithmetic mean of the chamber location. The CV between chambers

160   locations was calculated as the SD of the seventeen average fluxes per chamber location, divided by the arithmetic mean of the seventeen average fluxes per chamber location. Daily fluxes were calculated by taking the arithmetic mean of all measurements from all seventeen chamber locations for each day and the CV between days was calculated as the SD divided by the arithmetic mean of all daily fluxes. Annual budgets were calculated by adding the daily fluxes for one complete year. Days without flux measurements were filled using a linear interpolation if the gap was smaller than or equal to 10

165   consecutive days. For each of the ninety-five fast box chambers, an average flux was calculated by taking the arithmetic mean of all measurements from one chamber during the measurement period. These fluxes were then averaged per plot, and the CV for each plot was calculated as the SD divided by the mean of the average fluxes per chamber. To investigate the effect of potential drivers of GHG fluxes, i.e., WFPS, soil temperature, air temperature and precipitation, linear mixed models were fitted using the nlme package, version 3.1-164 (Pinheiro et al., 2023), with the measurements from the

170   automated chambers for each GHG. This was done using chamber number and collar numbers (i.e., location and position) as a random intercepts and WFPS, soil temperature ($Temp_{soil}$), air temperature ($Temp_{air}$), accumulated rainfall of the past 30 minutes (Rain) and accumulated rainfall of the past 10 days ($PrevRain_{10days}$) as fixed factors. To account for the temporal correlation in the data, a first order auto-regressive model was included in the fit (CorAR1). The CO_2 and N_2O fluxes were log-transformed and the CH_4 fluxes were log-transformed after adding the minimum value of the fluxes. Fixed factors were

175   removed from the fit if they had low t-values and removing them from the fit did not substantially increase the AIC and BIC values of the fit. R^2 values were calculated according to Nakagawa et al. (2013) and partitioned following Stoffel et al. (2021). Collinearity of predictors was tested using the variance of inflation factor (VIF). Effect sizes of the fixed factors are expressed as relative changes (%) in flux per unit increase in the fixed factor and are calculated by transforming the effect size y by $exp(y) - 1$. Note that for CH_4 this relative change is calculated as a function of fluxes with the minimum flux added.

180   Statistical difference between chamber locations for WFPS and soil temperature was tested with the Kruskal-Wallice test (nonparametric), followed by a Wilcox test. Statistical difference between hours for diel cycles was tested with the Friedman test (nonparametric, repeated measures), followed by a Wilcox test. Results were considered significant if the p-values or Bonferroni adjusted p-values were smaller than 0.05. To look into the effect of the high sampling frequency of the set-up, a resampling procedure was carried out with the daytime measurements to simulate lower sampling frequencies with the same

185   number of chambers by using a bootstrap with size 1000. The resampling scenarios were: a) one measurement per chamber every month, b) one measurement per chamber every week, and c) one measurement per chamber every day. The mean, minimum, maximum, interquartile range (IQR), and normalized interquartile range (NIQR) of the resulting budgets were calculated for each scenario. The NIQR was calculated as the IQR divided by the mean value and gives an indication of the spread of the resulting budgets, compared to the mean value. More information about the resampling procedure can be found

190   in the supplementary material. All statistical analyses were performed using R software.

4 Results

4.1 Climatic Variables

Total accumulated precipitation during the 16 month measuring period was 2181.7 mm, with highest weekly accumulated precipitation of 133.7 mm in early of September (week 36) of 2022, followed by week 44 in early November 2022 and week 16 around half of April 2023 (Fig. S3). November 2022 was the wettest month of the measurement period and December 2022, followed by May 2023 were the driest months (Table S3). June 2023 had twice the rainfall of June 2022, which made June 2023 a considerably wet month for the short dry season, while May 2023 was drier compared to May 2022. August and September 2023 were dry for the start of the long wet season, each having around half of the amount of rainfall than the same month in 2022. The average hourly air temperature was 23.8 ± 2.5°C with a hourly minimum of 17.8 °C during the night and a maximum of 32.3 °C during the day (Fig. S3).

Average WFPS at 5 cm depth was 27.8 ± 5.9 %, with an average soil temperature of 23.9 ± 0.6 °C, while average WFPS at 15 cm depth was 19.8 ± 4.1 % with an average soil temperature of 24.0 ± 0.5 °C. WFPS followed the seasonality of rainfall (Table S3) and ranged from a minimum at 5 cm and 15 cm of 11.3 % and 6.5 %, respectively, to a maximum of 69.9 % and 42 % (Fig. S4 and Table S5). Soil temperature ranged from a minimum at 5 cm and 15 cm of 21.7 °C and 21.9 °C, respectively, to a maximum of 26.1°C and 25.9°C (Fig. S4 and Table S4). A diel cycle marked soil temperature dynamics at both depths (Fig. S5). At both depths, there were pronounced differences in WFPS and soil temperature between chamber locations (Table S3).

4.2 Soil CO_2, CH_4 and N_2O exchange of automated chambers

CO_2 emissions from all chambers during the measurement period ranged from 37.2 to 463.1 mg C m^{-2} h^{-1} (Table S6) with an arithmetic mean, calculated with all measurements, of 174.5 ± 50.1 mg C m^{-2} h^{-1} and a median of 64.1 mg C m^{-2} h^{-1} (Fig. S6 a). Average emissions varied between chambers with lowest average emission of 124.4 mg C m^{-2} h^{-1} (chamber 8, collar 2) and highest average emission of 263.1 mg C m^{-2} h^{-1} (chamber 7, collar 1). Nevertheless, spatial variability over the entire measurement period appeared to be limited with a CV between chamber locations of 24 % (Table S6). The annual budgets, calculated for all 12 consecutive months ranged from 15.0 to 15.1 Mg C ha^{-1} yr^{-1} (Table S4).

The CH_4 flux during the measurement period ranged from -133.1 to 1209.0 µg C m^{-2} h^{-1} (Table S6) with an arithmetic mean, calculated with all measurements, of -44.6 ± 59.1 µg C m^{-2} h^{-1} and a median of -54. µg C m^{-2} h^{-1} (Fig. S6 b). Averaged over the entire measurement period, all chambers were a sink for CH_4 with average uptake rates ranging from -85.0 µg C m^{-2} h^{-1} (chamber 5, collar 1) to -19.2 µg C m^{-2} h^{-1} (chamber 7, collar 1). Although the forest soil was a sink, each chamber position except collar 1 of chamber 5 experienced at least one period of high CH_4 emissions (Table S6). Such an emission period had a duration of a couple of hours up to three weeks. In total 9.4 % of all CH_4 measurements were CH_4 sources, with maximum

per chamber location of 21 % (chamber 7, collar 1). The CV between chambers was 48 % indicating a strong spatial variability. The cumulative annual budgets ranged from an uptake of -3.7 to -4.1 kg C ha^{-1} yr^{-1} (Table S4).

225

The N_2O emissions during the measurement period ranged from 2.8 to 841.5 µg N m^{-2} h^{-1} (Table S6) with an arithmetic mean, calculated with all measurements, of 40.9 ± 46.4 µg N m^{-2} h^{-1} and a median of 25.4 µg N m^{-2} h^{-1} (Fig. S6 c). Averaged emissions per chamber ranged from 22.9 µg N m^{-2} h^{-1} (chamber 8, collar 2) up to 65.4 µg N m^{-2} h^{-1} (chamber 7, collar 2) and the relatively low CV of 30 %, indicates that the spatial variability was limited over this extended period (Table S6). A
230 cumulative annual budget for the N_2O measurements is not possible due to the three month data gap.

For CO_2, a diel cycle was observed with emissions increasing from 10:00 in the morning up to 14:00 and decreasing again from 17:00 to 21:00 (Fig. S7 a). For N_2O a small diel cycle was also observed with emissions increasing between 10:00 and 14:00 and decreasing again from 14:00 (Fig. S7 b). For CH_4 no diel cycle was observed (Fig. S7 c).

235

Daily fluxes were calculated by taking the arithmetic mean of all measurements from all nine chambers for each day. The mean daily flux for CO_2 was 174.0 ± 17.9 mg C m^{-2} h^{-1} (Fig. 1 a) with a CV between days of 10 % and a range from 103.5 to 227.7 mg C m^{-2} h^{-1}. The low CV of the daily fluxes and the low CV of each chamber location individually (13 % – 23 %, Table S6), indicate that the temporal variability for CO_2 was limited. The mean daily CH_4 flux was -44.7 ± 20.3 µg C m^{-2} h^{-1}
240 (Fig. 1 b) with a CV of 45 % and a range from -83.1 to 72.0 C m^{-2} h^{-1}. There were 11 days with a positive mean flux. These positive fluxes were mostly dominated by one or two chambers showing elevated emissions covering periods of several days. The CV of the daily averages, including all chambers, was relatively small compared to the CV of the individual chamber locations (23 % – 598 %, Table S6). The mean daily N_2O flux was 39.3 ± 27.7 µg N m^{-2} h^{-1} (Fig. 1 c) with a high CV of 70 % and a range of 5.1 to 135.6 µg N m^{-2} h^{-1}. The individual chamber locations also had high CV (56 % – 211 %,
245 Table S6).

Reducing the sampling frequency of the measurements per chamber to one measurement every month and one measurements every week, led to GHG budgets with a NIQR of 19.1 % and 9.1 %, respectively, for CH_4 and 13.6 % and 7.0 %, respectively, for N_2O, indicating a large spread of the calculated budgets (Table S10 and Fig. S8). All three scenario resulted
250 in relatively low NIQR values for CO_2. Resampling the data with one measurement per chamber per day resulted in a NIQR smaller than 3 % for all GHG.

4.3 Soil CO_2, CH_4 and N_2O exchange of fast box measurements

The average CO_2 flux of all ninety-five fast box chambers was 189.4 mg C m^{-2} h^{-1} (Table 1), a value close to the average of the nine automated chambers during the same period, 176.3 mg C m^{-2} h^{-1}. The CV between different plots was 9 % and the
255 CV between different chambers was 36 %, which was higher than the CV of 26 % between the automated chambers during

the month of August. For CH_4, the average uptake measured with the fast box method was -89.4 µg C m^{-2} h^{-1} with a CV of 42 %. Out of a total of 546 measurements for CH_4, sixteen measurements showed positive fluxes (3 %) distributed over eleven chambers in three different plots. Only one chamber had a positive flux over the entire measurement period. The average uptake rate measured with the fast box chambers was higher than the average uptake measured with the nine automated chambers in August, which was -58.8 µg C m^{-2} h^{-1}. The CV between the plots was 14 % and the CV between the fast box chambers was higher than the CV of the automated chambers during this period (35 %). For N_2O, the average flux was 95.5 µg N m^{-2} h^{-1} with a high CV of 73 % between the chambers and 24 % between the plots, indicating a large spatial variability. The average flux measured by the fast box chambers was much higher than the flux measured by the automated chambers throughout the whole measurement period. Due to a technical issue, the automated chambers have no flux measurements for N_2O during the month of August, however the average flux measured with the automated chambers in July and September 2023 is 23.9 µg N m^{-2} h^{-1} which is only a third of the value measured with the fast box chambers. The CV between the fast box chambers was much higher than the CV between the automated chambers in July and September (35 %).
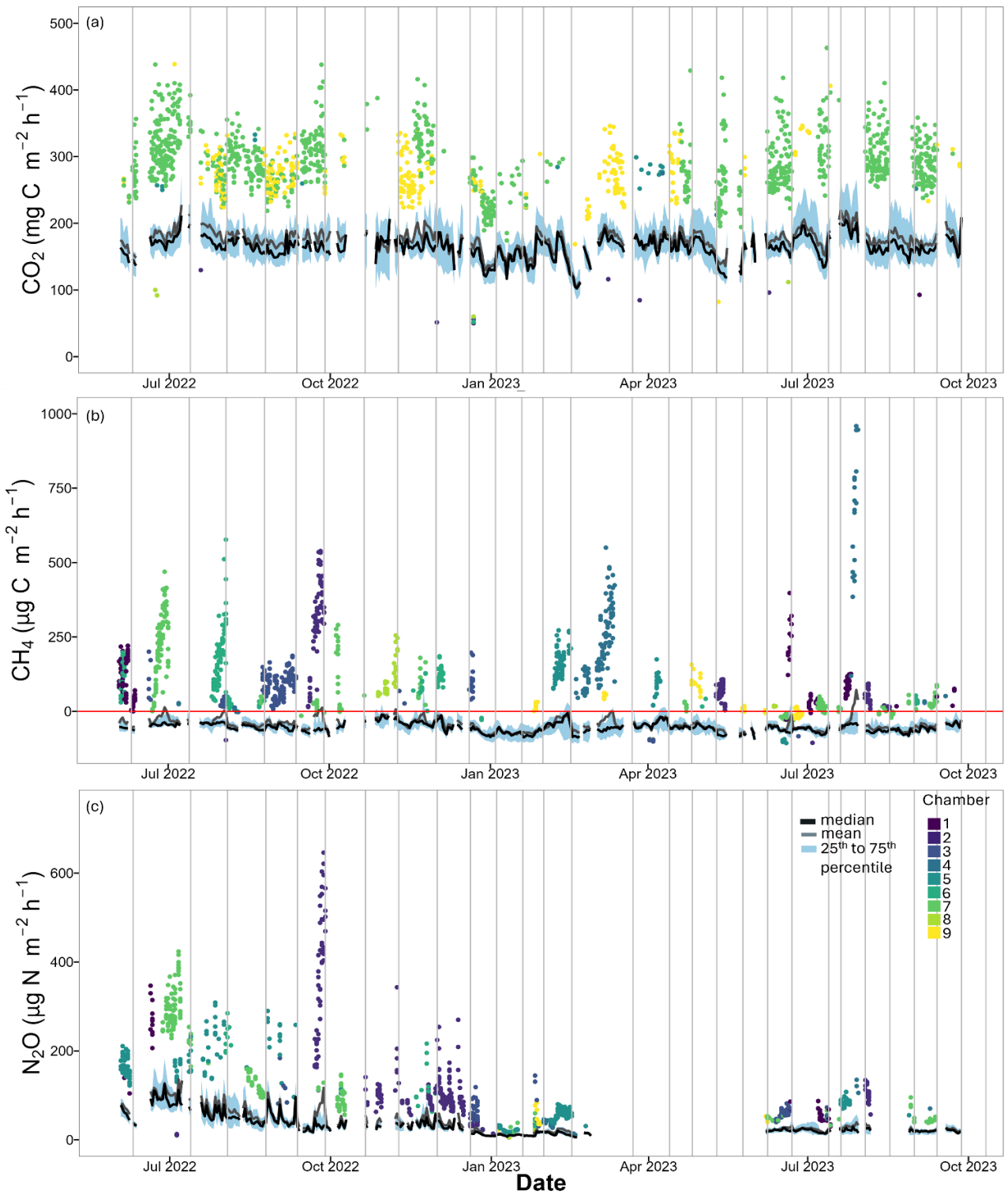
Figure 1: a) CO₂, b) CH₄ and c) N₂O fluxes of all nine _automated_ chambers over the whole measuring period. In black are the daily median values, in grey the daily averages, in blue the 25th up to 75th quantile and the coloured points are outlier values. Outliers have a distance to the 25th or 75th quantile value that is larger than 1.5 times the interquartile distance. Each colour represents one chamber. Vertical grey lines depict days where the chambers were replaced from one collar to the other.

Table 1: For each of fast box chambers an average flux is calculated using all measurements from that chamber during the measurement period. The values in this table are calculated using the average values per chamber. The average flux per plot for CO_2 (mg C m^{-2} h^{-1}), CH_4 (µg C m^{-2} h^{-1}) and N_2O (µg N m^{-2} h^{-1}) together with the minimum and maximum value ($mean \, ^{max}_{min}$) and the coefficient of variation (CV). Also the mean and CV is calculated for all fast box chambers together and for the averages of the 4 plots.

Plot	CO_2 (mg C m^{-2} h^{-1})	CH_4 (µg C m^{-2} h^{-1})	N_2O (µg N m^{-2} h^{-1})
CF1	$201.9\,^{470}_{60}$	$-87.8\,^{-22}_{-150}$	$83.8\,^{171}_{32}$
	CV: 0.41	CV: 0.41	CV: 0.45
CF2	$203.2\,^{321}_{90}$	$-105.2\,^{-49}_{-167}$	$101.5\,^{241}_{32}$
	CV: 0.30	CV: 0.30	CV: 0.53
Mi2	$166.3\,^{271}_{81}$	$-90.1\,^{40}_{-146}$	$70.8\,^{364}_{22}$
	CV: 0.27	CV: 0.46	CV: 1.04
Mi5	$18\text{43.69}\,^{403}_{71}$	$-74.4\,^{-2}_{-141}$	$124.2\,^{397}_{45}$
	CV: 0.39	CV: 0.48	CV: 0.76
All	189.4	-89.4	95.5
chambers	CV: 0.36	CV 0.42	CV: 0.73
All plots	188.8	-89.4	95.1
	CV: 0.09	CV 0.14	CV: 0.24

4.3 Main Drivers of the GHG fluxes

For CO_2, all fixed factors were retained and all had a positive relationships with CO_2 fluxes (Fig. 2 a and b, Table S7). The fixed and random factors together explained up to 79 % of the variance of the fluxes. Similarly, only positive relationships were found between N_2O emissions and climatic variables (Fig. 2 c and d, Table S9). Rain was removed from the fit and all effects together explained 22 % of the variability. For CH_4, all effects together explained 35 % of the variability. Both rainfall and soil temperature were removed from the fit. A positive relationship with CH_4 was found for WFPS and a negative relationship for air temperature (Fig. 2 e and f, Table S8). The model did not fit the data of the CH_4 measurements well, as the residuals showed heteroscedasticity and non-normality. WFPS has the largest relative effect size within the range of variability for all three models Fig.2 b, d and f). The VIF for all predictors in all models were less than two.
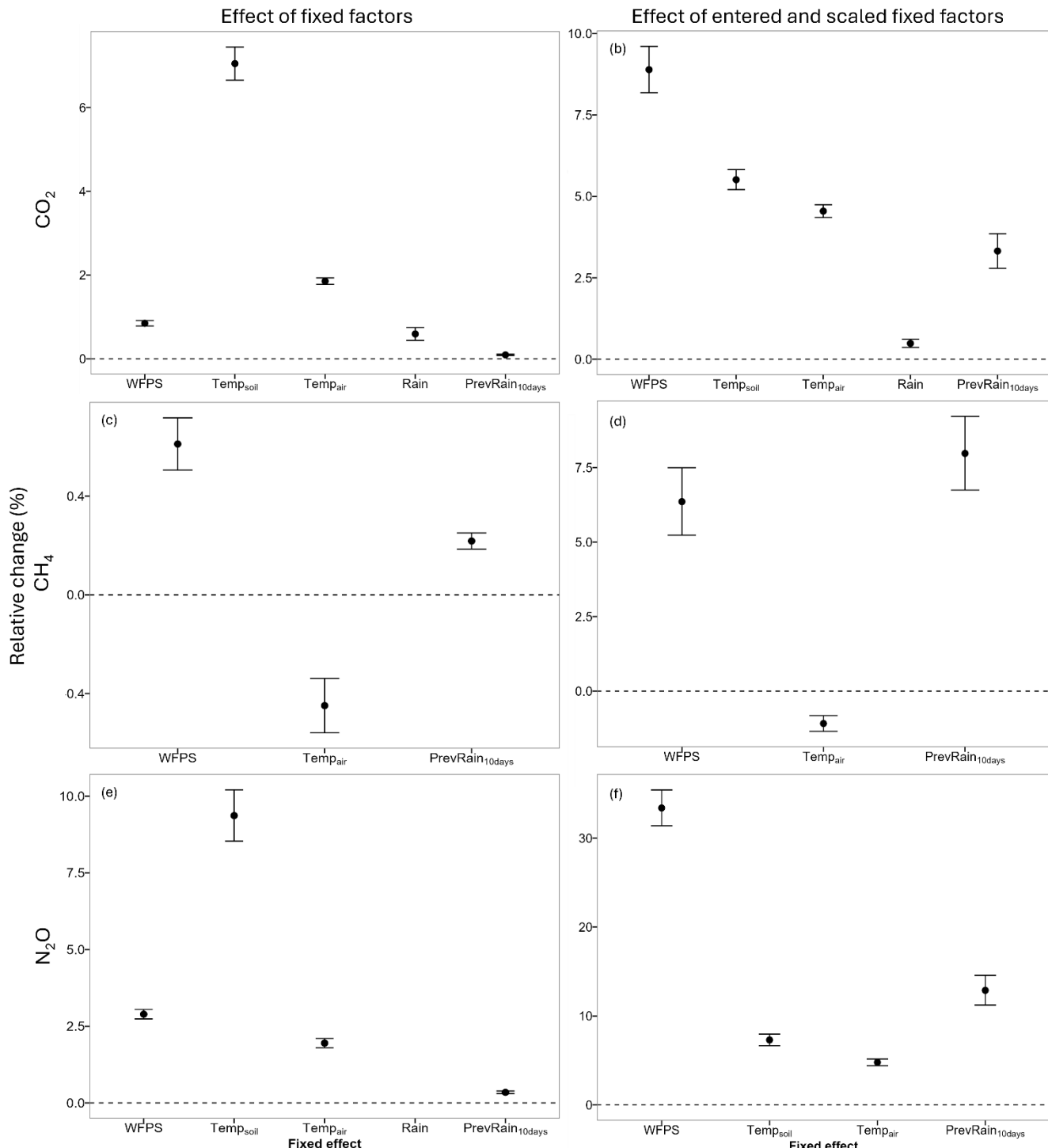
Figure 2: The relative fixed effect sizes (%) for the fixed factors and the centred and scaled fixed factors water filled pore space (WFPS, %), soil temperature (Temp$_{soil}$, °C), air temperature (Temp$_{air}$, °C), precipitation (Rain, mm per half hour) and the accumulated precipitation of the previous 10 days (PrevRain$_{10days}$, mm) for the linear mixed effect models of the automated chamber measurements of the three greenhouse gasses a) CO$_2$, b) CO$_2$ with centred and scaled fixed factors, c) CH$_4$, d) CH$_4$ with centred and scaled fixed factors, e) N$_2$O and f) N$_2$O with centred and scaled fixed factors. The whiskers indicate the 95% credible interval.

285

5 Discussion

5.1 Soil CO₂ emission

The average of all the measurements from the automated chambers results in a carbon emission of 15.3 ± 4.4 Mg C ha^{-1} yr^{-1}. The gap filled daily fluxes accumulated to an annual budget of 15.1 Mg C ha^{-1} yr^{-1} (Table S4). This value is higher than the previous estimate of 13.1 Mg C ha^{-1} yr^{-1} by Baumgartner et al. (2020) in the DRC, and more than double the amount of 6.3 Mg C ha^{-1} yr^{-1} estimated by Werner et al. (2007) in Kenya. Our values are close to the 17.0 and 18.3 Mg C ha^{-1} yr^{-1} estimated by Tchiofo Lontsi et al. (2020) for an undisturbed forest area in Cameroon. Our study shows that this Congolese forest soil is a larger CO_2 source than observed for tropical forest soils in French Guiana, with an emissions between 9.3 and 13.6 Mg C ha^{-1} yr^{-1} (Courtois et al. 2018; Petitjean et al. 2019) and in Australia with emissions between 8 and 12 Mg C ha^{-1} yr^{-1} (Kiese et al. 2002). However, the emissions are comparable to those measured in Brazil, between 13.2 and 16.3 Mg C ha^{-1} yr^{-1} (Sotta et al., 2007; Sousa Neto et al., 2011) and lower than the emissions reported for forests in Panama with 19.7 Mg C ha^{-1} yr^{-1} (Pendall et al., 2010).

In this study, there was a low spatial variability between the automated chambers and between the fast box chambers and also a low temporal variability for CO_2 fluxes. This was also observed in other lowland tropical forests in Kenya by Werner et al. (2006) and in the DRC by Baumgartner et al. (2020). This WFPS, soil and air temperature were the strongest drivers, each explaining up to 8% of the variability in the data (Table S7). The random effect 'chamber ID', accounted for a large proportion of the variance. Both WFPS and soil temperature had a positive relationship with CO_2 flux, with WFPS having a larger relative effect size than soil temperature within their range of variability (centred and scaled factors) (Fig. 2). The positive relationship with WFPS is frequently observed in other studies, both in the Congo Basin and in other topical forests. During the early wetter period in July 2022, a first emission peak was observed with an increase of WFPS. However, there is a slight decline in the following wet months although WFPS remains high (Fig. S9 a). The same was observed in forests in Panama, where the decrease in emissions was partly attributed to a depletion of readily available C substrates and nutrients (Cusack et al. 2023). Baumgartner et al. (2020) suggest that CO_2 emissions in lowland forests in the Congo Basin may be limited by C availability, which could explain the decline in emissions after the first pulse of microbial activity pulse at the beginning of the rainy season. A clear decrease in CO_2 emissions is also observed from the start of the drier period in mid-November 2022. The following relatively large peaks in emissions align with the increase in WFPS due to sporadic rain events. These emission peaks following rewetting events are common and are referred to as the 'Birch effect' (Birch, 1958). With an increasing length of the dry season as expected from climate change predictions for the Congo Basin (Jiang et al., 2019), soil CO_2 emissions may decrease. However, with increasing rainfall intensity, which is also part of climate change projections (Kasongo Yakusu et al., 2023), the emission pulses after rewetting could become more frequent and severe. The positive relationship with soil and air temperature can explain the diel cycle of the CO_2 emissions found in this study (Fig.

S5 and Fig. S7 a). Peak soil respiration is reached before the peak of soil temperature, which indicates that the diel cycle is also sustained by increasing autotrophic respiration (Savage et al. 2013; Winnick et al. 2020).

320 **5.2 Soil CH$_4$ uptake**

For CH$_4$, the total uptake is -3.9 kg C ha^{-1} yr^{-1} when using the arithmetic mean of all the measurements from the automated chambers and the annual budgets accumulate to an uptake between -3.7 and 4.1 kg C ha^{-1} yr^{-1} (Table S4). This uptake is close to estimates from previous studies in the DRC with an uptake of -3.5 kg C ha^{-1} yr^{-1} (Barthel et al., 2022), but is higher than the average uptake rate of tropical forest soils of -2.5 kg C ha^{-1} yr^{-1} estimated by Dutaur et al. (2007) and -3.0 kg C ha^{-1}

325 yr^{-1} estimated by Dalal et al. (2008). In other African tropical forests similar uptake rates were reported, e.g. Cameroon -4.3 and -2.5 kg C ha^{-1} yr^{-1} (Tchiofo Lontsi et al., 2020) and -3.5 kg C ha^{-1} yr^{-1} (Macdonald et al., 1998) and Kenya -4.9 kg C ha^{-1} yr^{-1} (Werner et al. 2007). Uptake rates of -2.6 kg C ha^{-1} yr^{-1} were measured in Southwest China (Werner et al., 2006), -3.2 kg C ha^{-1} yr^{-1} in Australia (Kiese et al., 2003), -3.8 kg C ha^{-1} yr^{-1} in Brazil (Sousa Neto et al., 2011) and -1.1 kg C ha^{-1} yr^{-1} in French Guiana (Petitjean et al., 2019).

330

Considerable spatial variability was observed with a CV of 47 % and 42 % between the automated and the fast box chambers respectively. The average uptake measured with the fast box method was -89.4 µg C m^{-2} h^{-1} with a range of all measurements separately of -230.8 to 256.99 µg C m^{-2} h^{-1}, while during the same period, the automated chambers measured an average flux of -66.8 µg C m^{-2} h^{-1} with a range of -162.8 to 272.2 µg C m^{-2} h^{-1}. This discrepancy may indicate that the nine automated

335 chambers are not sufficient to cover the considerable spatial variability of CH$_4$ uptake, underlining the importance of a large spatial coverage. The CV of the daily averages (45 %) was relatively small compared to the CV of the individual chamber locations (Table S6), indicating that the temporal variability of the daily fluxes of all chambers together was relatively small, but that each chamber individually had a large temporal variability, mainly caused by the periods of emissions. This high spatial and temporal variability is commonly found in studies in tropical forests (Barthel et al., 2022; Castaldi et al., 2020;

340 Werner et al., 2007). Resampling the automated chamber measurements with a lower sampling frequency of once a month or once a week, results in a large spread of possible CH$_4$ budgets (Table S10 and Fig. S8) which underlines the importance of a high sampling frequency.

The long-standing theory is that microbial methanogenesis can only occur in anoxic soils. Consequently, most weathered

345 tropical forest soils are modelled as CH$_4$ sinks. However, sporadic CH$_4$ emissions have been measured in several studies. In the study by Werner et al. (2007), high WFPS together with crumbled soil structure, suggesting termite activity, were put forward as a possible explanation. Termite activity was also mentioned to explain CH$_4$ emissions in the study by Barthel et al. (2022). In a study in Costa-Rica by Calvo-Rodriguez et al. (2020), high methane emissions were associated with heavy precipitation events. While in the study by Castaldi et al. (2020), emissions were observed in well-drained soils and the

350 authors suggested that the emissions may have been generated by anoxic hotspots of microbial activity within the overall

aerobic soil. In this study, no clear evidence of termite activity was found at the chamber locations. The WFPS during emission periods ranged from 13.5 % up to 70.5 % (Table S5), so the emissions did not occur only during wetter periods (Fig S9 b). In the case that the emissions are triggered by heavy precipitation events, one would expect multiple chambers to emit during the same period, but in this study the timing of substantial CH_4 emissions was different for all chambers. Even though WFPS and accumulated rainfall were the strongest drivers in the model, they explained only up to 4.8 % of the variability (Table S8). Overall, this suggests that the emissions in our study are also associated with sporadic anoxic microsites, controlled by methanogenesis, as suggested by Castaldi et al. (2020) (Angle et al., 2017; Lacroix et al., 2023; Teh et al., 2005). A positive relation between the flux and WFPS was found, which is frequently mentioned in other studies (Kiese et al. 2003; Werner et al. 2006; Werner et al. 2007; Sousa Neto et al. 2011) and a negative relationship between the flux and soil and air temperature was found, however the relationship with soil temperature was insignificant.

5.3 Soil N_2O emission

The arithmetic mean of all measurements results in a budget of 3.6 kg N yr^{-1} ha^{-1}. This value is close to the emission of 3.8 kg N ha^{-1} yr^{-1} measured in Kenya (Werner et al. 2007). However the value is higher than tropical average of 3 kg N ha^{-1} yr^{-1} estimated by Dalal et al. (2008), more than double of the emissions measured previously in DRC using static chambers, 1.6 kg N ha^{-1} yr^{-1} (Barthel et al., 2022) or measured in Cameroon 1.6 kg N ha^{-1} yr^{-1} (Iddris et al., 2020). The value is also higher than the 2.3 kg N ha^{-1} yr^{-1} estimated for Ghana (Castaldi et al. 2013) and the 2.9 kg N ha^{-1} yr^{-1} estimated for the Mayombe Forest in Congo (Serca et al., 1994). The emissions from the CongoFlux site are also higher than several other measurements in tropical forests as the 0.5 kg N ha^{-1} yr^{-1} estimated in southwestern China (Werner et al., 2006), 2.4 kg N ha^{-1} yr^{-1} estimated in the eastern Amazonia (Verchot et al., 1999), 1.0 kg N ha^{-1} yr^{-1} in French Guiana (Petitjean et al., 2019) and 1.0, 4.4 and 7.5 kg N ha^{-1} yr^{-1} in Australia (Kiese et al. 2002; Kiese et al. 2003).

The N_2O emissions have a high temporal variability, as the automated chambers have coefficients of variation between 56 % and 211 % (Table S6). Lowering the sampling frequency, resulted in large spread of possible N_2O budgets (Table 10 and Fig. S8) reducing the accuracy and precision of the estimated budgets (Barton et al., 2015). Emission change significantly from year to year. The same months separated by only one year can differ in N_2O emissions by a factor of four. This high temporal variability is consistent with most studies in tropical forests. In Australia two consecutive years of measurements in the same region differed in N_2O emission by a factor of seven (Kiese et al. 2002; Kiese et al. 2003). The CV between the fast box measurements is high (73 %) which supports the high spatial variability of N_2O emissions (Barthel et al., 2022; Castaldi et al., 2013; Werner et al., 2007). The average flux of the fast box chambers during the three weeks in August 2023 is twice as high as the average flux measured by the nine automated chambers during the entire measurement period and three time as high as the average flux measured by the automated chambers in July and September 2023. The large discrepancy between the measured fluxes from automated and fast box measurements together with the low CV between the automated

chambers, but the high CV between the fast box chambers, may indicate that the nine automated chambers are not able to capture to full spatial heterogeneity of the N_2O emissions.

385 WFPS is the strongest driver (Table S9) and has the largest relative effect size within its range of variability compared to other predictors (Fig. 2). The positive relationships fitted by the linear mixed model isare found in several studies, confirming higher emissions during wet season, compared to dry seasons (Iddris et al., 2020; Werner et al., 2007). Shortly after rain events, N_2O emissions increase rapidly and then slowly decrease slowly again with decreasing WFPS (Fig. S9 c). From January 2023, with the onset of the drier months, the high fluxes and peaked responses to increasing WFPS seem to

390 disappear. This phenomenon was also observed by Kiese et al. (2003) in Australia, where it could have been associated with significant changes in the composition of the microbial community. With the onset of the early wet season around June and July, the emissions do not increase again. However, the fast box flux in August is almost the same as the high average flux measured by the automated chambers around the same period in the previous year (June and July 2022). The large difference could therefore also in some extend be the result of altered conditions- -at the chamber locations due to the long deployment

395 of the automated chambers aton the same location. However there was no clear difference for the other GHG fluxes during this period and the location of the automated chambers was consistently changed between collars, so this effect should be minor. The relatively low marginal R² of the fit suggests that there are other main drivers responsible for the large temporal variability in N_2O emissions. Other potential drivers could be soil pH, microbial community composition, nutrient availability, … (Butterbach-Bahl et al., 2013) however in this study, we did not investigate these as sampling for the

400 mentioned other drivers, even only at a weekly frequency, was not trivial nor feasible.

6 Conclusions

Despite being the second largest tropical forest worldwide, the Congo Basin is still generally understudied. The little available soil GHG flux data has a diversity of measurement techniques and resulting GHG budgets. In this study, a combination of automated and manual fast box chamber measurements was used, to quantify and understand the

405 spatiotemporal variability of soil GHG fluxes in a semi-deciduous tropical forest in the Congo Basin. The CongoFlux site is in terms of vegetation representative for around 33 % of the entire basin, assuming a total size of 3.6 million square kilometer (Shapiro et al., 2021). Moreover, the forest type found on the site represent 91 % of all forest types in the Basin. According to (Baert et al., (2009), the main soil type of the CongoFlux site (Ferrasols) is also the dominant soil type in the DRC. We therefore believe that the results of this study provide a robust estimate, representative for a large area within the

410 Congo Basin.

Overall, our observations confirm that tropical forest soils are a major source of CO_2 and N_2O and a sink for CH_4. With an emission of 15.1 Mg C ha^{-1} yr^{-1}, this study identifies the soil of this study area in the Congo Basin as a larger CO_2 source than most tropical forest soils previously reported in the literature. For N_2O, the emissions at the CongoFlux site were also higher than most emissions previously measured at tropical sites. With a global warming potential 265 times greater than

415 CO_2, these high N_2O emissions should be taken into account in the GHG budget of tropical forests. Large spatial and temporal variability was found for the CH_4 and N_2O fluxes, highlighting the need for additional measurement campaigns in the Congo Basin with an experimental design allowing importance of large spatial coverage and particularly high temporal sampling frequency when measuring soil fluxes. Lowering the sampling frequency of the measurements leads to a decline in precisions of the estimated budgets. Soil and air temperature are positively related to CO_2 and N_2O emissions. Therefore, an
420 increasing number of warm days and nights and general warmer weather conditions could lead to overall higher CO_2 and N_2O emissions from soils. CO_2 and N_2O emissions are lowest during drier periods, therefore, the increasing length of dry season could offset the effect of the increasing emissions with increasing temperatures. However, there are clear spikes in N_2O emissions after rainfall events and higher CO_2 emissions after the onset of the rainy season, and with an increasing precipitation intensity, this could lead to higher and more frequent emission peaks for both CO_2 and N_2O, which in turn
425 would increase the total GHG emissions from tropical forest soils. An increasing precipitation intensity could also lead to less uptake of CH_4, lowering the net uptake of -3.9 kg C ha^{-1} yr^{-1} found in this study, but with the lower global warming potential of CH_4, this will only have a small influence on the total GHG emissions from forest soil. The net effect of climate change on the GHG budget of this ecosystem is still hard to predict and should be further investigated with appropriate warming and controlled rainfall studies.

430

Code availability

Code will be made available upon request.

Data availability

The core datasets generated during the current study have been deposited in the Zenodo repository
435 [10.5281/zenodo.12200453] and are also available from the corresponding author upon request.

Supplement link

Author contribution

R. Daelman, M. Bauters and P. Boeckx conceived the study. R. Daelman, E. Bulonza, L. Lefevre., D.E., F.K., and J. Mbifo., H.F., M.B., L.C. and H.V. conducted the fieldwork. K. Butterbach-Bahl, R. Kiese and B. Wolf designed the automated
440 chamber setup and the code to calculate the fluxes. R. Daelman did the statistical data analysis. All co-authors substantively revised the manuscript.

Competing interests

The authors declare that they have no conflict of interest.

Acknowledgements

445 The authors thank the CongoFlux team (L. Lefevre, D. Ekili, F. Kimbesa, H. Fundji, J. Mbifo) and S. Bodé for assisting in the installation, the fieldwork and for the maintenance of the chamber set up and thank master students L. Ceulemans and H. Verbruggen for assisting with the manual chamber measurements. We thank F. Van Damme for all organizational assistance and the local community in Yangambi and all Congolese friends who drove us, cooked for us and helped us navigate the forest. We further acknowledge the support by the Institut National des Etudes et Recherches Agronomique (INERA) during

450 our fieldwork in the Yangambi Biosphere Reserve and by ICOS (Integrated Carbon Observation System).

References

Aguilar, E., Aziz Barry, A., Brunet, M., Ekang, L., Fernandes, A., Massoukina, M., Mbah, J., Mhanda, A., do Nascimento, D. J., Peterson, T. C., Thamba Umba, O., Tomou, M., and Zhang, X.: Changes in temperature and precipitation extremes in western central Africa, Guinea Conakry, and Zimbabwe, 1955–2006, J. Geophys. Res. Atmospheres, 114,

455 https://doi.org/10.1029/2008JD011010, 2009.

Anderson-Teixeira, K. J., Wang, M. M. H., McGarvey, J. C., and LeBauer, D. S.: Carbon dynamics of mature and regrowth tropical forests derived from a pantropical database (TropForC-db), Glob. Change Biol., 22, 1690–1709, https://doi.org/10.1111/gcb.13226, 2016.

Angle, J. C., Morin, T. H., Solden, L. M., Narrowe, A. B., Smith, G. J., Borton, M. A., Rey-Sanchez, C., Daly, R. A.,

460 Mirfenderesgi, G., Hoyt, D. W., Riley, W. J., Miller, C. S., Bohrer, G., and Wrighton, K. C.: Methanogenesis in oxygenated soils is a substantial fraction of wetland methane emissions, Nat. Commun., 8, 1567, https://doi.org/10.1038/s41467-017-01753-4, 2017.

Arias-Navarro, C., Díaz-Pinés, E., Zuazo, P., Rufino, M. C., Verchot, L. V., and Butterbach-Bahl, K.: Quantifying the contribution of land use to N2O, NO and CO2 fluxes in a montane forest ecosystem of Kenya, Biogeochemistry, 134, 95–

465 114, https://doi.org/10.1007/s10533-017-0348-3, 2017.

Baert, G., Van Ranst, E., Ngongo, M., Kasongo, E., Verdoodt, A., Mujinya, B. B., and Mukalay, J.: Guide des sols en République Démocratique du Congo, tome II: description et données physico-chimiques de profils types, 2009.

Barthel, M., Bauters, M., Baumgartner, S., Drake, T. W., Bey, N. M., Bush, G., Boeckx, P., Botefa, C. I., Dériaz, N., Ekamba, G. L., Gallarotti, N., Mbayu, F. M., Mugula, J. K., Makelele, I. A., Mbongo, C. E., Mohn, J., Mandea, J. Z.,

470 Mpambi, D. M., Ntaboba, L. C., Rukeza, M. B., Spencer, R. G. M., Summerauer, L., Vanlauwe, B., Van Oost, K., Wolf, B., and Six, J.: Low N2O and variable CH4 fluxes from tropical forest soils of the Congo Basin, Nat. Commun., 13, https://doi.org/10.1038/s41467-022-27978-6, 2022.

Barton, L., Wolf, B., Rowlings, D., Scheer, C., Kiese, R., Grace, P., Stefanova, K., and Butterbach-Bahl, K.: Sampling frequency affects estimates of annual nitrous oxide fluxes, Sci. Rep., 5, 15912, https://doi.org/10.1038/srep15912, 2015.

475   Baumgartner, S., Barthel, M., William Drake, T., Bauters, M., Ahanamungu Makelele, I., Kalume Mugula, J., Summerauer, L., Gallarotti, N., Cizungu Ntaboba, L., Van Oost, K., Boeckx, P., Doetterl, S., Anton Werner, R., and Six, J.: Seasonality, drivers, and isotopic composition of soil CO_2 fluxes from tropical forests of the Congo Basin, Biogeosciences, 17, 6207–6218, https://doi.org/10.5194/bg-17-6207-2020, 2020.

Birch, H. F.: The effect of soil drying on humus decomposition and nitrogen availability, Plant Soil, 10, 9–31,
480   https://doi.org/10.1007/BF01343734, 1958.

Bréchet, L. M., Daniel, W., Stahl, C., Burban, B., Goret, J. Y., Salomón, R. L., and Janssens, I. A.: Simultaneous tree stem and soil greenhouse gas (CO_2, CH_4, N_2O) flux measurements: a novel design for continuous monitoring towards improving flux estimates and temporal resolution, New Phytol., 230, 2487–2500, https://doi.org/10.1111/nph.17352, 2021.

Brookshire, E. N. J., Gerber, S., Menge, D. N. L., and Hedin, L. O.: Large losses of inorganic nitrogen from tropical
485   rainforests suggest a lack of nitrogen limitation, Ecol. Lett., 15, 9–16, https://doi.org/10.1111/j.1461-0248.2011.01701.x, 2012.

Butterbach-Bahl, K., Baggs, E. M., Dannenmann, M., Kiese, R., and Zechmeister-Boltenstern, S.: Nitrous oxide emissions from soils: How well do we understand the processes and their controls?, Philos. Trans. R. Soc. B Biol. Sci., 368, https://doi.org/10.1098/rstb.2013.0122, 2013.

490   Calvin, K., Dasgupta, D., Krinner, G., Mukherji, A., Thorne, P. W., Trisos, C., Romero, J., Aldunce, P., Barrett, K., Blanco, G., Cheung, W. W. L., Connors, S., Denton, F., Diongue-Niang, A., Dodman, D., Garschagen, M., Geden, O., Hayward, B., Jones, C., Jotzo, F., Krug, T., Lasco, R., Lee, Y.-Y., Masson-Delmotte, V., Meinshausen, M., Mintenbeck, K., Mokssit, A., Otto, F. E. L., Pathak, M., Pirani, A., Poloczanska, E., Pörtner, H.-O., Revi, A., Roberts, D. C., Roy, J., Ruane, A. C., Skea, J., Shukla, P. R., Slade, R., Slangen, A., Sokona, Y., Sörensson, A. A., Tignor, M., Van Vuuren, D., Wei, Y.-M., Winkler,
495   H., Zhai, P., Zommers, Z., Hourcade, J.-C., Johnson, F. X., Pachauri, S., Simpson, N. P., Singh, C., Thomas, A., Totin, E., Arias, P., Bustamante, M., Elgizouli, I., Flato, G., Howden, M., Méndez-Vallejo, C., Pereira, J. J., Pichs-Madruga, R., Rose, S. K., Saheb, Y., Sánchez Rodríguez, R., Ürge-Vorsatz, D., Xiao, C., Yassaa, N., Alegría, A., Armour, K., Bednar-Friedl, B., Blok, K., Cissé, G., Dentener, F., Eriksen, S., Fischer, E., Garner, G., Guivarch, C., Haasnoot, M., Hansen, G., Hauser, M., Hawkins, E., Hermans, T., Kopp, R., Leprince-Ringuet, N., Lewis, J., Ley, D., Ludden, C., Niamir, L., Nicholls, Z., Some,
500   S., Szopa, S., Trewin, B., Van Der Wijst, K.-I., Winter, G., Witting, M., Birt, A., Ha, M., et al.: IPCC, 2023: Climate Change 2023: Synthesis Report. Contribution of Working Groups I, II and III to the Sixth Assessment Report of the Intergovernmental Panel on Climate Change [Core Writing Team, H. Lee and J. Romero (eds.)]. IPCC, Geneva, Switzerland., Intergovernmental Panel on Climate Change (IPCC), https://doi.org/10.59327/IPCC/AR6-9789291691647, 2023.

505   Calvo-Rodriguez, S., Kiese, R., and Sánchez-Azofeifa, G. A.: Seasonality and Budgets of Soil Greenhouse Gas Emissions From a Tropical Dry Forest Successional Gradient in Costa Rica, J. Geophys. Res. Biogeosciences, 125, e2020JG005647, https://doi.org/10.1029/2020JG005647, 2020.

Castaldi, S., Bertolini, T., Valente, A., Chiti, T., and Valentini, R.: Nitrous oxide emissions from soil of an African rain forest in Ghana, Biogeosciences, 10, 4179–4187, https://doi.org/10.5194/bg-10-4179-2013, 2013.

510   Castaldi, S., Bertolini, T., Nicolini, G., and Valentini, R.: Soil Is a Net Source of Methane in Tropical African Forests, FORESTS, 11, 1157, https://doi.org/10.3390/f11111157, 2020.

Chaney, N. W., Sheffield, J., Villarini, G., and Wood, E. F.: Development of a High-Resolution Gridded Daily Meteorological Dataset over Sub-Saharan Africa: Spatial Analysis of Trends in Climate Extremes, J. Clim., 27, 5815–5835, https://doi.org/10.1175/JCLI-D-13-00423.1, 2014.

515   Courtois, E. A., Stahl, C., Van den Berge, J., Bréchet, L., Van Langenhove, L., Richter, A., Urbina, I., Soong, J. L., Peñuelas, J., and Janssens, I. A.: Spatial Variation of Soil CO2, CH4 and N2O Fluxes Across Topographical Positions in Tropical Forests of the Guiana Shield, Ecosystems, 21, 1445–1458, https://doi.org/10.1007/s10021-018-0232-6, 2018.

Courtois, E. A., Stahl, C., Burban, B., Van den Berge, J., Berveiller, D., Bréchet, L., Soong, J. L., Arriga, N., Peñuelas, J., and Janssens, I. A.: Automatic high-frequency measurements of full soil greenhouse gas fluxes in a tropical forest,
520   Biogeosciences, 16, 785–796, https://doi.org/10.5194/bg-16-785-2019, 2019.

Cusack, D. F., Dietterich, L. H., and Sulman, B. N.: Soil Respiration Responses to Throughfall Exclusion Are Decoupled From Changes in Soil Moisture for Four Tropical Forests, Suggesting Processes for Ecosystem Models, Glob. Biogeochem. Cycles, 37, e2022GB007473, https://doi.org/10.1029/2022GB007473, 2023.

Dalal, R. C. and Allen, D. E.: Greenhouse gas fluxes from natural ecosystems, Aust. J. Bot., 56, 369,
525   https://doi.org/10.1071/BT07128, 2008.

Dezfuli, A.: Climate of Western and Central Equatorial Africa, in: Oxford Research Encyclopedia of Climate Science, https://doi.org/10.1093/acrefore/9780190228620.013.511, 2017.

Dutaur, L. and Verchot, L. V.: A global inventory of the soil CH4 sink, Glob. Biogeochem. Cycles, 21, https://doi.org/10.1029/2006GB002734, 2007.

530   Gilson, R., Van Wambeke, A. and Gutzwiller, R.: Carte Des Sols Et De La Végétation Du Congo Belge Et Du Ruanda-Urundi. Brussels, Belgium:L'Institut National pour l'Etude Agronomique du Congo Belge (I.N.E.A.C.), 1956.

Hedin, L. O., Brookshire, E. N. J., Menge, D. N. L., and Barron, A. R.: The Nitrogen Paradox in Tropical Forest Ecosystems, Annu. Rev. Ecol. Evol. Syst., 40, 613–635, https://doi.org/10.1146/annurev.ecolsys.37.091305.110246, 2009.

Hensen, A., Skiba, U., and Famulari, D.: Low cost and state of the art methods to measure nitrous oxide emissions, Environ.
535   Res. Lett., 8, 025022, https://doi.org/10.1088/1748-9326/8/2/025022, 2013.

Iddris, N. A. A., Corre, M. D., Yemefack, M., van Straaten, O., and Veldkamp, E.: Stem and soil nitrous oxide fluxes from rainforest and cacao agroforest on highly weathered soils in the Congo Basin, Biogeosciences, 17, 5377–5397, https://doi.org/10.5194/bg-17-5377-2020, 2020.

Jiang, Y., Zhou, L., Tucker, C. J., Raghavendra, A., Hua, W., Liu, Y. Y., and Joiner, J.: Widespread increase of boreal
540   summer dry season length over the Congo rainforest, Nat. Clim. Change, 9, 617–622, https://doi.org/10.1038/s41558-019-0512-y, 2019.

Karam, S., Seidou, O., Nagabhatla, N., Perera, D., and Tshimanga, R. M.: Assessing the impacts of climate change on climatic extremes in the Congo River Basin, Clim. Change, 170, 40, https://doi.org/10.1007/s10584-022-03326-x, 2022.

Kasongo Yakusu, E., Van Acker, J., Van deVyver, H., Bourland, N., Ndiapo, J., Likwela, T., Kipifo, M., Kankolongo, A.,
545   Van den Bulcke, J., Beeckman, H., Bauters, M., Boeckx, P., Verbeeck, H., Jacobsen, K., Demarée, G., Gellens-Meulenberghs, F., and Hubau, W.: Ground-based climate data show evidence of warming and intensification of the seasonal rainfall cycle during the 1960–2020 period in Yangambi, central Congo Basin, Clim. Change, 176, https://doi.org/10.1007/s10584-023-03606-0, 2023.

Kendon, E. J., Stratton, R. A., Tucker, S., Marsham, J. H., Berthou, S., Rowell, D. P., and Senior, C. A.: Enhanced future
550   changes in wet and dry extremes over Africa at convection-permitting scale, Nat. Commun., 10, 1794, https://doi.org/10.1038/s41467-019-09776-9, 2019.

Kiese, R. and Butterbach-Bahl, K.: N2O and CO2 emissions from three different tropical forest sites in the wet tropics of Queensland, Australia, Soil Biol. Biochem., 34, 975–987, https://doi.org/10.1016/S0038-0717(02)00031-7, 2002.

Kiese, R. and Butterbach-Bahl, K.: N2O and CO2 emissions from three different tropical forest sites in the wet tropics of Queensland, Australia, n.d.

Kiese, R., Hewett, B., Graham, A., and Butterbach-Bahl, K.: Seasonal variability of N_2O emissions and CH_4 uptake by tropical rainforest soils of Queensland, Australia: SEASONALITY OF N_2O AND CH_4 FLUXES IN TROPICAL RAINFORESTS, Glob. Biogeochem. Cycles, 17, n/a-n/a, https://doi.org/10.1029/2002GB002014, 2003.

Lacroix, E. M., Aeppli, M., Boye, K., Brodie, E., Fendorf, S., Keiluweit, M., Naughton, H. R., Noël, V., and Sihi, D.: Consider the Anoxic Microsite: Acknowledging and Appreciating Spatiotemporal Redox Heterogeneity in Soils and Sediments, ACS Earth Space Chem., 7, 1592–1609, https://doi.org/10.1021/acsearthspacechem.3c00032, 2023.

Likoko, Mbifo, Besango, Totiwe, Badjoko, D., Likoko, A. G., Botomo, A. D., Litemandia, Yn, Alongo, L. S., and Boyemba, B.: Climate Change for Yangambi Forest Region , DR Congo, 2019.

Macdonald, J. A., Eggleton, PauL., Bignell, D. E., Forzi, F., and Fowler, D.: Methane emission by termites and oxidation by soils, across a forest disturbance gradient in the Mbalmayo Forest Reserve, Cameroon, Glob. Change Biol., 4, 409–418, https://doi.org/10.1046/j.1365-2486.1998.00163.x, 1998.

Malhi, Y., Adu-Bredu, S., Asare, R. A., Lewis, S. L., and Mayaux, P.: African rainforests: past, present and future, Philos. Trans. R. Soc. B Biol. Sci., 368, 20120312, https://doi.org/10.1098/rstb.2012.0312, 2013.

Marthews, T., D, M., Y, M., Phillips, O., W, H.-H., Riutta, T., Ruiz-Jaen, M., C, G., R, U., Butt, N., R, C., and Oliveras, I.: Measuring Tropical Forest Carbon Allocation and Cycling: A RAINFOR-GEM Field Manual for Intensive Census Plots, 2013.

Nakagawa, S. and Schielzeth, H.: A general and simple method for obtaining R2 from generalized linear mixed-effects models, Methods Ecol. Evol., 4, 133–142, https://doi.org/10.1111/j.2041-210x.2012.00261.x, 2013.

Ni, X. and Groffman, P. M.: Declines in methane uptake in forest soils, Proc. Natl. Acad. Sci., 115, 8587–8590, https://doi.org/10.1073/pnas.1807377115, 2018.

Pendall, E., Schwendenmann, L., Rahn, T., Miller, J. B., Tans, P. P., and White, J. W. C.: Land use and season affect fluxes of CO2, CH4, CO, N2O, H2 and isotopic source signatures in Panama: evidence from nocturnal boundary layer profiles, Glob. Change Biol., 16, 2721–2736, https://doi.org/10.1111/j.1365-2486.2010.02199.x, 2010.

Petitjean, C., Le Gall, C., Pontet, C., Fujisaki, K., Garric, B., Horth, J.-C., Hénault, C., and Perrin, A.-S.: Soil N2O, CH4, and CO2 Fluxes in Forest, Grassland, and Tillage/No-Tillage Croplands in French Guiana (Amazonia) Soil N_2O, CH_4, and CO_2 Fluxes in Forest, Grassland, and Tillage/No-Tillage Croplands in French Guiana (Amazonia) Chambre d'Agriculture de Guyane, 97333 Cayenne CEDEX, Guyane française, Tillage Crop. Fr. Guiana Amazon. Soil Syst., 3, 29, https://doi.org/10.3390/soilsystems3020029ï, 2019.

Pinheiro, J., Bates, D., to 2002), S. D. (up, to 2005), D. S. (up, authors (src/rs.f), E., sigma), S. H. (Author fixed, sigma), B. V. W. (Programmer fixed, Ranke (varConstProp()), J., and R Core Team: nlme: Linear and Nonlinear Mixed Effects Models, 2023.

Raich, J. W., Potter, C. S., and Bhagawati, D.: Interannual variability in global soil respiration, 1980–94, Glob. Change Biol., 8, 800–812, https://doi.org/10.1046/j.1365-2486.2002.00511.x, 2002.

Savage, K., Davidson, E. A., and Tang, J.: Diel patterns of autotrophic and heterotrophic respiration among phenological stages, Glob. Change Biol., 19, 1151–1159, https://doi.org/10.1111/gcb.12108, 2013.

Serca, D., Delmas, R., Jambert, C., and Labroue, L.: Emissions of nitrogen oxides from equatorial rain forest in central Africa:, Tellus B Chem. Phys. Meteorol., 46, 243–254, https://doi.org/10.3402/tellusb.v46i4.15795, 1994.

Shapiro, A. C., Grantham, H. S., Aguilar-Amuchastegui, N., Murray, N. J., Gond, V., Bonfils, D., and Rickenbach, O.: Forest condition in the Congo Basin for the assessment of ecosystem conservation status, Ecol. Indic., 122, 107268, https://doi.org/10.1016/j.ecolind.2020.107268, 2021.

Sibret, T., Bauters, M., Bulonza, E., Lefevre, L., Cerutti, P. O., Lokonda, M., Mbifo, J., Michel, B., Verbeeck, H., and Boeckx, P.: CongoFlux – The First Eddy Covariance Flux Tower in the Congo Basin, Front. Soil Sci., 2, 883236, https://doi.org/10.3389/fsoil.2022.883236, 2022.

Sotta, E. D., Veldkamp, E., Schwendenmann, L., Guimarães, B. R., Paixão, R. K., Ruivo, M. de L. P., LOLA da COSTA, A. C., and Meir, P.: Effects of an induced drought on soil carbon dioxide (CO2) efflux and soil CO2 production in an Eastern Amazonian rainforest, Brazil, Glob. Change Biol., 13, 2218–2229, https://doi.org/10.1111/j.1365-2486.2007.01416.x, 2007.

Sousa Neto, E., Carmo, J. B., Keller, M., Martins, S. C., Alves, L. F., Vieira, S. A., Piccolo, M. C., Camargo, P., Couto, H. T. Z., Joly, C. A., and Martinelli, L. A.: Soil-atmosphere exchange of nitrous oxide, methane and carbon dioxide in a gradient of elevation in the coastal Brazilian Atlantic forest, Biogeosciences, 8, 733–742, https://doi.org/10.5194/bg-8-733-2011, 2011.

Stoffel, M. A., Nakagawa, S., and Schielzeth, H.: partR2: partitioning R2 in generalized linear mixed models, PeerJ, 9, e11414, https://doi.org/10.7717/peerj.11414, 2021.

Tchiofo Lontsi, R., Corre, M. D., Iddris, N. A., and Veldkamp, E.: Soil greenhouse gas fluxes following conventional selective and reduced-impact logging in a Congo Basin rainforest, Biogeochemistry, 151, 153–170, https://doi.org/10.1007/s10533-020-00718-y, 2020.

Teh, Y. A., Silver, W. L., and Conrad, M. E.: Oxygen effects on methane production and oxidation in humid tropical forest soils, Glob. Change Biol., 11, 1283–1297, https://doi.org/10.1111/j.1365-2486.2005.00983.x, 2005.

Tian, H., Xu, R., Canadell, J. G., Thompson, R. L., Winiwarter, W., Suntharalingam, P., Davidson, E. A., Ciais, P., Jackson, R. B., Janssens-Maenhout, G., Prather, M. J., Regnier, P., Pan, N., Pan, S., Peters, G. P., Shi, H., Tubiello, F. N., Zaehle, S., Zhou, F., Arneth, A., Battaglia, G., Berthet, S., Bopp, L., Bouwman, A. F., Buitenhuis, E. T., Chang, J., Chipperfield, M. P., Dangal, S. R. S., Dlugokencky, E., Elkins, J. W., Eyre, B. D., Fu, B., Hall, B., Ito, A., Joos, F., Krummel, P. B., Landolfi, A., Laruelle, G. G., Lauerwald, R., Li, W., Lienert, S., Maavara, T., MacLeod, M., Millet, D. B., Olin, S., Patra, P. K., Prinn, R. G., Raymond, P. A., Ruiz, D. J., van der Werf, G. R., Vuichard, N., Wang, J., Weiss, R. F., Wells, K. C., Wilson, C., Yang, J., and Yao, Y.: A comprehensive quantification of global nitrous oxide sources and sinks, Nature, 586, 248–256, https://doi.org/10.1038/s41586-020-2780-0, 2020.

Vargas, R., Carbone, M. S., Reichstein, M., and Baldocchi, D. D.: Frontiers and challenges in soil respiration research: from measurements to model-data integration, Biogeochemistry, 102, 1–13, https://doi.org/10.1007/s10533-010-9462-1, 2011.

Verchot, L. V., Davidson, E. A., Cattânio, J. H., Ackerman, I. L., Erickson, H. E., and Keller, M.: Land use change and biogeochemical controls of nitrogen oxide emissions from soils in eastern Amazonia, Glob. Biogeochem. Cycles, 13, 31–46, https://doi.org/10.1029/1998GB900019, 1999.

Wangari, E. G., Mwanake, R. M., Kraus, D., Werner, C., Gettel, G. M., Kiese, R., Breuer, L., Butterbach-Bahl, K., and Houska, T.: Number of Chamber Measurement Locations for Accurate Quantification of Landscape-Scale Greenhouse Gas Fluxes: Importance of Land Use, Seasonality, and Greenhouse Gas Type, J. Geophys. Res. Biogeosciences, 127, e2022JG006901, https://doi.org/10.1029/2022JG006901, 2022.

630   Werner, C., Zheng, X., Tang, J., Xie, B., Liu, C., Kiese, R., and Butterbach-Bahl, K.: N2O, CH4 and CO2 emissions from seasonal tropical rainforests and a rubber plantation in Southwest China, Plant Soil, 289, 335–353, https://doi.org/10.1007/s11104-006-9143-y, 2006.

Werner, C., Kiese, R., and Butterbach-Bahl, K.: Soil-atmosphere exchange of N2O, CH4 and CO2 and controlling environmental factors for tropical rain forest sites in western Kenya, J. Geophys. Res. Atmospheres, 112,
635   https://doi.org/10.1029/2006JD007388, 2007.

Winnick, M. J., Lawrence, C. R., McCormick, M., Druhan, J. L., and Maher, K.: Soil Respiration Response to Rainfall Modulated by Plant Phenology in a Montane Meadow, East River, Colorado, USA, J. Geophys. Res. Biogeosciences, 125, e2020JG005924, https://doi.org/10.1029/2020JG005924, 2020.